LA-UR- 97-38

*Approved for public release; distribution is unlimited.*

Title: DIAMOND: A GRAPHICAL INTERFACE TOOLBOX FOR COMPARATIVE MODAL ANALYSIS AND DAMAGE IDENTIFICATION

CONF-970736--2

Author(s): Scott W. Doebling, ESA-EA, MS P946
Charles A. Farrar, ESA-EA, MS P946
Phillip J. Cornwell, ESA-EA, MS P946
(Affiliate)

Submitted to: Sixth International Conference on Recent Advances in Structural Dynamics, 14-17 July 1997, Southampton, England



## DISCLAIMER



Los Alamos
NATIONAL LABORATORY

# DIAMOND: A Graphical Interface Toolbox for Comparative Modal Analysis and Damage Identification

Scott W. Doebling[1], Charles R. Farrar[2]

*Los Alamos National Laboratory*
*Los Alamos, NM, 87545*
*USA*

Phillip J. Cornwell[3]

*Rose Hulman Institute of Technology*
*5500 Wabash Ave.*
*Terre Haute, IN, 47805*
*USA*

**Abstract**

This paper introduces a new toolbox of graphical-interface software algorithms for the numerical simulation of vibration tests, analysis of modal data, finite element model correlation, and the comparison of both linear and nonlinear damage identification techniques. This toolbox is unique because it contains several different vibration-based damage identification algorithms, categorized as those which use only measured response and sensor location information ("non-model-based" techniques) and those which use finite element model correlation ("model-based" techniques). Another unique feature of this toolbox is the wide range of algorithms for experimental modal analysis. The toolbox also contains a unique capability that utilizes the measured coherence functions and Monte Carlo analysis to perform statistical uncertainty analysis on the modal parameters and damage identification results. This paper contains a detailed description of the var-

---

[1]Technical Staff Member, Engineering Sciences and Applications Division, Engineering Analysis Group (ESA-EA), M/S P946, (505) 667-6950, doebling@lanl.gov

[2]Technical Staff Member, Engineering Sciences and Applications Division, Engineering Analysis Group (ESA-EA)

[3]Associate Professor, Dept. of Mechanical Engineering

ious modal analysis, damage identification, and model correlation capabilities of toolbox, and also shows a sample application which uses the toolbox to analyze the statistical uncertainties on the results of a series of modal tests performed on a highway bridge.

## INTRODUCTION

This paper introduces a new suite of graphical-interface software algorithms to numerically simulate vibration tests and to apply various modal analysis, damage identification, and finite element model refinement techniques to measured or simulated modal vibration data. This toolbox is known as DIAMOND (Damage Identification And MOdal aNalysis for Dummies), and has been developed at Los Alamos National Laboratory over the last year. DIAMOND is written in MATLAB [1], a numerical matrix math application which is available on all major computer platforms. DIAMOND is unique in three primary ways:

1. DIAMOND contains several of the most widely used modal curve-fitting algorithms. Thus the user may analyze the data using more than one technique and compare the results directly. This modal identification capability is coupled with a numerical test-simulation capability that allows the user to directly explore the effects of various test conditions on the identified modal parameters.

2. The damage identification and finite element model refinement modules are graphically interactive, so the operation is intuitive and the results are displayed visually as well as numerically. This feature allows the user to easily interpret the results in terms of structural damage.

3. DIAMOND has statistical analysis capability built into all three major analysis modules: modal analysis, damage identification, and finite element model refinement. The statistical analysis capability allows the user to determine the magnitude of the uncertainties associated with the results. No other software package for modal analysis or damage identification has this capability.

The development of DIAMOND was motivated primarily by the lack of graphical implementation of modern damage identification and finite element model refinement algorithms. Also, the desire to have a variety of

modal curve-fitting techniques available and the capability to generate numerical data with which to compare the results of each technique was a motivating factor. The authors are unaware of any commercial software package that integrates all of these features.

This paper is organized as follows: An overview of DIAMOND is provided, including an outline of each module (except for the numerical test simulator): experimental modal analysis and statistical analysis of modal data, damage identification, and finite element model updating. In each section, a flowchart of the menu structure of DIAMOND is presented. Following the overview section is an example of the application of DIAMOND to vibration data obtained from an actual highway bridge. This section contains a detailed description of the testbed, data acquisition equipment, and testing procedure. It also contains a sample experimental modal analysis, complete with statistical analysis of the variability of the results with respect to the variations inherent in the data acquisition process as well as variations resulting from changes in the environmental conditions of the bridge.

## OVERVIEW OF DIAMOND

DIAMOND is divided into four primary modules at the top level: numerical vibration test simulator, experimental modal curve fitting and statistical analysis, damage identification, and structural dynamic model updating. These four modules constitute the primary hierarchy in DIAMOND, as shown in Figure 1. In this paper, the three analysis-oriented

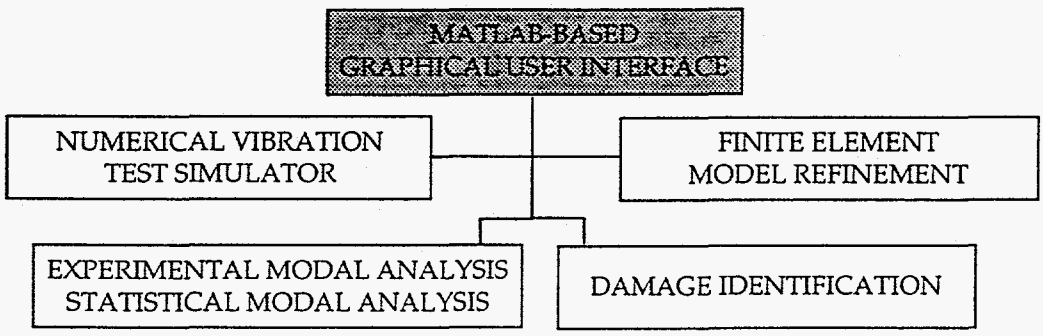


**Figure 1: Flowchart of Top Level of DIAMOND**

modules (all but the test simulator) will be discussed in further detail.

Experimental Modal Analysis / Statistical Analysis of Modal Data

The experimental modal analysis module provides a series of tools for plotting the data in various forms, plotting data indicator functions, defining sensor geometry, performing modal curve-fits, analyzing the results of modal curve fits, and analyzing the variance of identified modal parameters as a function of the noise in the measurements as defined by the measured coherence function. A flowchart of this module is shown in Figure 2.

The most important feature of the experimental modal analysis module is the variety of modal parameter identification algorithms which are available. These include:

1. Operating shapes (which is simply "peak picking," or "slicing" the FRF matrix at a particular frequency bin)

2. Eigensystem Realization Algorithm (ERA), [2] which is a low-order time domain modal parameter estimation algorithm.

3. Complex exponential algorithm, which is a high-order time domain modal parameter estimation algorithm. The specific algorithm implemented is the Polyreference Time Domain [3] approach.

4. Rational Polynomial Curve fit [4], which is a high-order frequency domain technique that uses orthogonal polynomials to estimate the coefficients of a rational polynomial representation of the frequency response function.

5. Nonlinear least squares fit is a frequency domain parameter estimation technique that uses a Levenberg-Marquardt nonlinear least-squares curve fitting routine [5] to estimate modal frequencies and modal damping ratios from the unfiltered Fourier spectral responses of a base-excited structure.

Any of these modal identification algorithms can be implemented in a statistical Monte Carlo [6] technique. In such an analysis, a series of perturbed data sets, based on the statistics of the measured FRFs as defined by the measured coherence functions, are generated and propagated through the selected algorithm. The statistics on the results are then used as uncertainty bounds on the identified modal parameters.

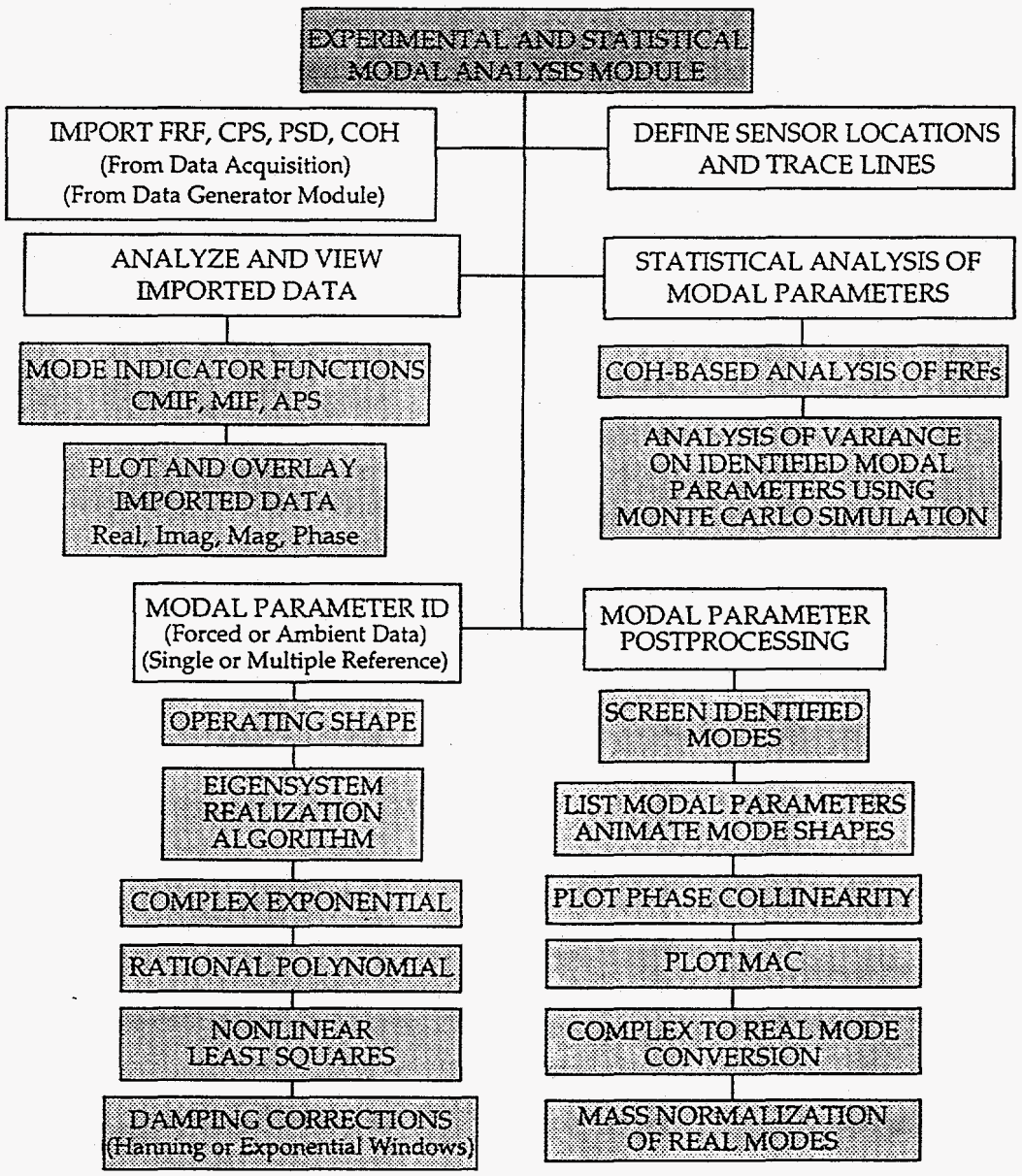


**Figure 2: Flowchart of Experimental Modal Analysis / Statistical Modal Analysis Module**

Damage Identification

The algorithms contained in the damage identification module of DIAMOND can be classified as modal-based, finite element refinement-based, or nonlinear. A flowchart of the damage identification module is shown in

Figure 3.

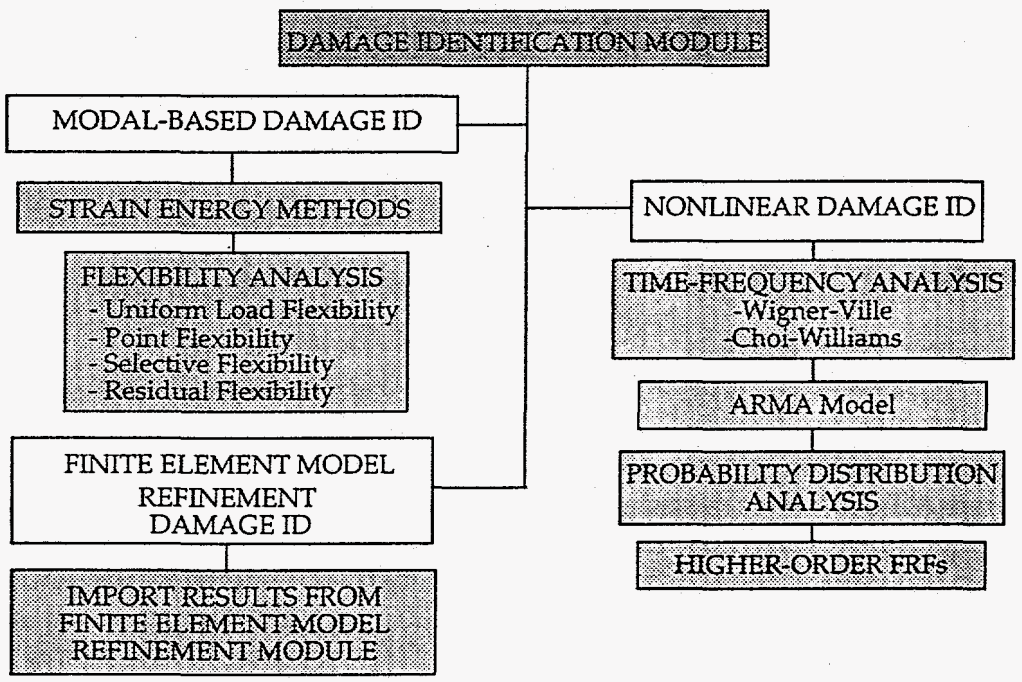


**Figure 3: Flowchart of Damage Identification Module**

The damage identification module presents a number of different algorithms:

1. Strain energy methods are based on the work of Stubbs [7], Cornwell [8], and others. The basic idea of these methods is the division of the structure into a series of beam or plate-like elements, and then the estimation of the strain energy stored in each element both before and after damage. The curvatures (second-derivatives with respect to space) of the mode shapes are used to approximate the strain energy content.

2. Flexibility methods all use some measure of the change in the modal flexibility matrix, estimated from the mass-normalized measured mode shapes, $[\Phi]$, and modal frequencies squared, $[\Lambda]$, as

$$[G] \approx [\Phi][\Lambda]^{-1}[\Phi]^T \tag{1}$$

The modal flexibility matrix is used to estimate the static displacement the structure would undergo as a result of a specified loading pattern. The uniform load flexibility method [9] involves specifying a unit load at all measurement degrees of freedom (DOF), then comparing the change in the resulting displacement pattern before and after damage. The point flexibility method [10] specifies the application of a unit load at each measurement DOF one at a time, then looking for a change in the resulting displacements at the same point before and after damage.

The selective flexibility method, which is still under development, uses one of the above two flexibility approaches but filters the modes used to form the flexibility matrix according to their relative statistical uncertainty. The idea of this method is to exclude modes with a high uncertainty from the analysis to avoid biasing the results.

The residual flexibility method [11] also uses one of the above two flexibility approaches but includes the estimate of the residual flexibility, which is the contribution to the flexibility matrix from the modes above the bandwidth of interest. The resulting flexibility matrix is a closer approximation to the true static flexibility matrix than is the modal flexibility matrix.

3. Finite element model correlation-based damage identification techniques are based on the comparison of the finite element model correlation results from before damage to those after damage. The correlation techniques are discussed in the next section.

4. Nonlinear damage identification techniques are based on different theories of nonlinear signal processing. They are a widely varying group of methods and are reviewed and discussed in Ref. [12].

Finite Element Model Refinement

The finite element model refinement module consists of four options: pre-processing for update analysis, optimal matrix updating, sensitivity-based model update, and post-processing of update results. A flowchart of this module is shown in Figure 4.

The pre-processing phase of the model correlation analysis involves the selection of which modal parameters (i.e. modal frequencies and mode shapes) should be used in the correlation, as well as which finite element

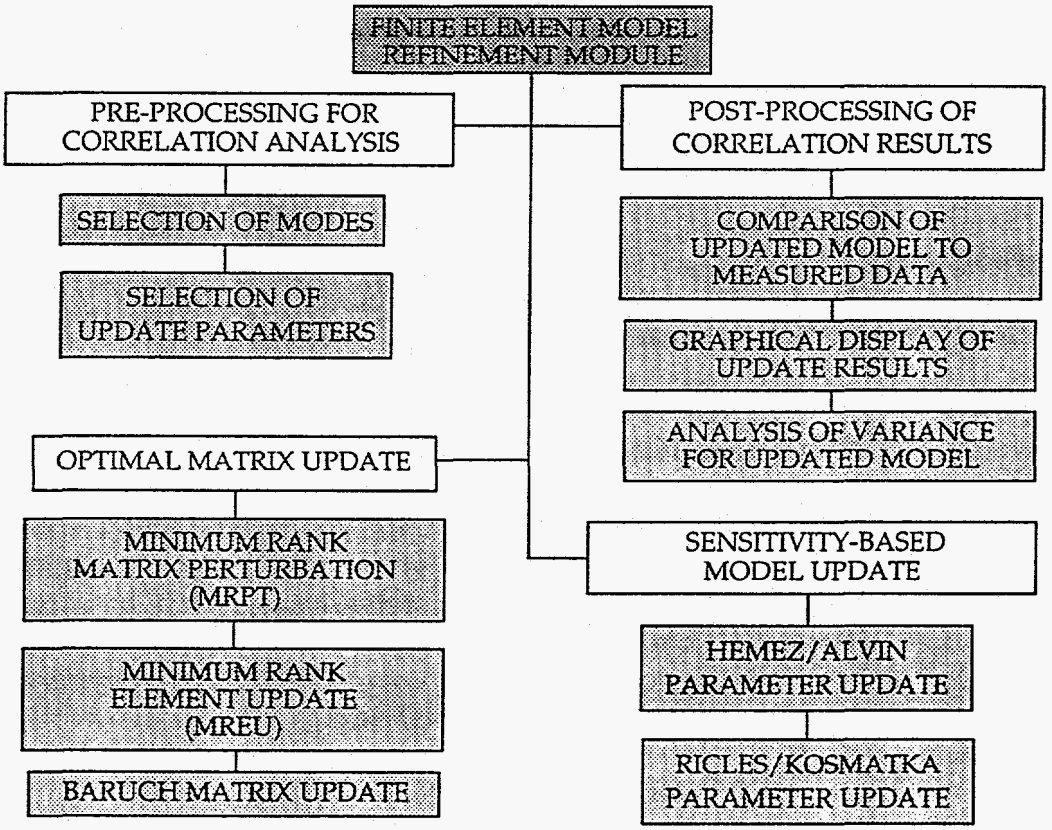


**Figure 4: Flowchart of Finite Element Model Refinement Module**

model parameters should be updated.

The optimal matrix update methods are based on the minimization of the error in the structural eigenproblem using a closed-form, direct solution. The minimum rank perturbation technique (MRPT) [13] is one such method which produces a minimum-rank perturbation of the structural stiffness, damping, and/or mass matrices reduced to the measurement degrees of freedom. The minimum rank element update (MREU) [14] is a similar technique which produces perturbations at the elemental, rather than the matrix, level. The Baruch updating technique [15] minimizes an error function of the eigenequation using a closed-form function of the mass and stiffness matrices.

The sensitivity-based model update methods also seek to minimize the error in the structural eigenequation, but do so using a Newton-Raphson-type technique based on solving for the perturbations such that the gradient

of the error function is near zero. [6] Thus these methods require the computation of the sensitivity of the structural eigenproblem to the parameters which are to be updated. The Hemez/Alvin algorithm [16],[17] computes the sensitivities at the elemental level, then assembles them to produce the global sensitivity matrices. The Ricles/Kosmatka [18] algorithm computes a "hybrid" sensitivity matrix using both analytical and experimental sensitivities.

## EXAMPLE APPLICATION: THE ALAMOSA CANYON BRIDGE

The following analysis of modal data from a series of tests performed on a highway bridge is intended to demonstrate the application of the unique capabilities of DIAMOND to data from an actual field test.

The Alamosa Canyon Bridge has seven independent spans with a common pier between successive spans. An elevation view of the bridge is shown in Figure 5. The bridge is located on a seldom-used frontage road

**Figure 5: Elevation View of the Alamosa Canyon Bridge**

parallel to Interstate 25 about 10 miles North of the town of Truth or Consequences, New Mexico, USA. Each span consists of a concrete deck support-

ed by six W30x116 steel girders. The roadway in each span is approximately 7.3 m (24 ft) wide and 15.2 (50 ft) long. Integrally attached to the concrete deck is a concrete curb and concrete guard rail. Inspection of the bridge showed that the upper flanges of the beams are imbedded in the concrete, which implies the possibility of composite action between the girders and the deck. Between adjacent beams are four sets of cross braces equally spaced along the length of the span. The cross braces are channel sections (C12x25). A cross section of the span at a location showing the interior cross braces is shown in Figure 6. At the pier the beams rest on rollers, and at the abutment the beams are bolted to a half-roller to approximate a pinned connection. These end conditions are shown in Figure 7.

The data acquisition system used in the vibration tests consisted of a Toshiba TECRA 700 laptop computer, four Hewlett Packard (HP) 35652A input modules that provide power to the accelerometers and perform analog to digital conversion of the accelerometer signals, an HP 35651A signal processing module that performs the needed fast Fourier transform calculations, and a commercial data acquisition/signal analysis software package produced by HP. A 3500 watt GENERAC Model R-3500 XL AC generator was used to power this system.

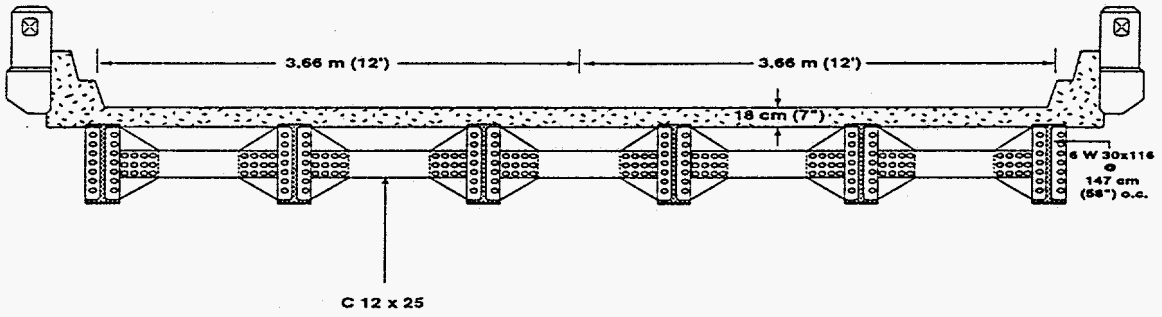


**Figure 6: Cross-Section of Alamosa Canyon Bridge Span**


**Figure 7: End Conditions of Alamosa Canyon Bridge Span**

The data acquisition system was set up to measure acceleration and force time histories and to calculate frequency response functions (FRFs), power spectral densities (PSDs), cross-power spectra and coherence functions. Sampling parameters were specified that calculated the FRFs from a 16-s time window discretized with 2048 samples. The FRFs were calculated for a frequency range of 0 to 50 Hz at a frequency resolution of 0.0625 Hz. A Force window was applied to the signal from the hammer's force transducer and exponential windows were applied to the signals from the accelerometers. AC coupling was specified to minimize DC offsets.

A PCB model 086B50 impact sledge hammer was used as the impact excitation source. The hammer weighed approximately 53.4 N (12 lbs) and had a 7.6-cm-dia. (3-in-dia) steel head. This hammer has a nominal sensitivity of 0.73 mV/lb and a peak amplitude range of 5000 lbs. A Wilcoxon Research model 736T accelerometer was used to make the driving point acceleration response measurement adjacent to the hammer impact point. This accelerometer has a nominal sensitivity of 100 mV/g, a specified frequency range of 5 - 15,000 Hz, and a peak amplitude range of 50 g. PCB model 336c integrated circuit piezoelectric accelerometers were used for the vibration measurements. These accelerometers have a nominal sensitivity of 1 V/g, a specified frequency range of 1 - 2000 Hz, and an amplitude range of 4 g. More details regarding the instrumentation can be found in Ref. [19].

A total of 31 acceleration measurements were made on the concrete deck and on the girders below the bridge as shown in Figure 8. Five accelerome-

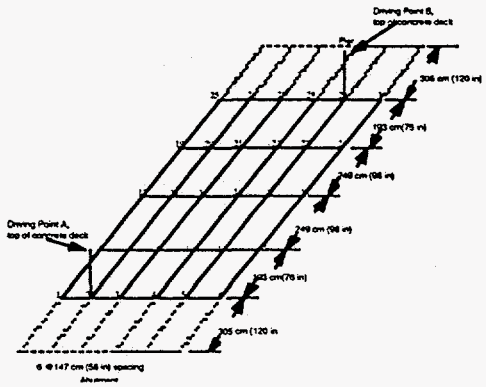

**Figure 8: Accelerometer and Impact Locations**

ters were spaced along the length of each girder. Because of the limited number of data channels, measurements were not made on the girders at

the abutment or at the pier. Two excitations points were located on the top of the concrete deck. Point A was used as the primary excitation location. Point B was used to perform a reciprocity check. The force-input and acceleration-response time histories obtained from each impact were subsequently transformed into the frequency domain so that estimates of the PSDs, FRFs, and coherence functions could be calculated. Thirty averages were typically used for these estimates. With the sampling parameters listed above and the overload reject specified, data acquisition for a specific test usually occurred over a time period of approximately 30 - 45 minutes. All of the results in this paper are from measurements made on span 1 of the bridge, which is located at the far North end.

A total of 52 data sets were collected over the course of the six days of testing. Temperature measurements were made at 9 locations around the bridge, both above and below the deck, to track the effects of ambient temperature changes on the test results. Reciprocity and linearity checks were conducted first. A series of modal tests was conducted over a 24 hour period (one test every 2 hours) to assess the change in modal properties as a result of variations in ambient environmental conditions, as discussed in Ref. [19]. A series of tests with various levels of attempted damage was also conducted, but the permitted alterations in the bridge did not cause a significant change in the measured modal properties. Specifically, the nuts on the bolted connections that hold the channel-section cross members to the girders, as shown in Figure 9 were removed. However the bolts could not be loos-

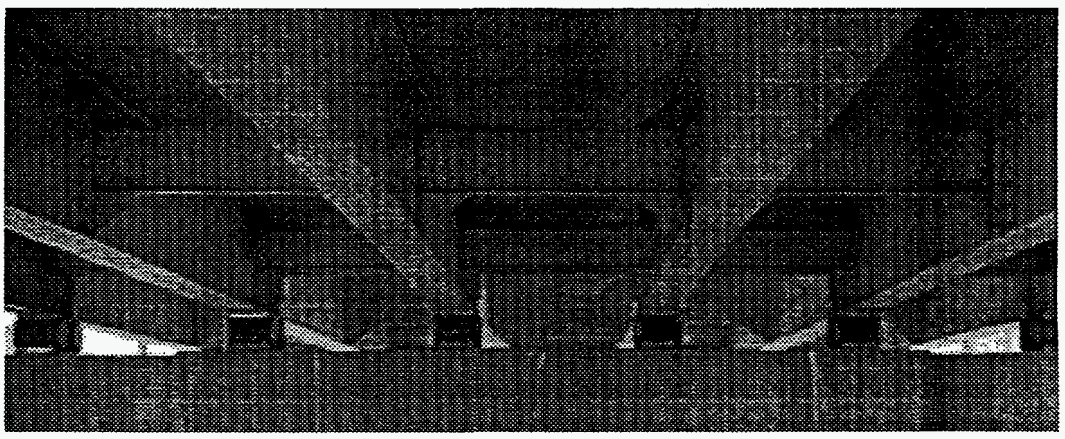

**Figure 9: Bolted Connections of Cross-Members to Girders**

ened sufficiently, and no relative motion could be induced at the interface under the loading of the modal excitation. For this reason, the damage cases

presented in this paper are results from simulated stiffness reduction using a correlated FEM.

## Identification of Modal Parameters from Modal Data

The identified modal frequencies and modal damping ratios from this analysis are shown in Table 1. The mode shapes identified in this analysis are shown in Figure 10.

**Table 1. Identified Modal Parameters from Alamosa Canyon Bridge Test**

| Mode Number | Modal Frequency (Hz) | Modal Damping Ratio (%) |
|---|---|---|
| 1 | 7.372 | 1.63% |
| 2 | 8.043 | 1.84% |
| 3 | 11.677 | 1.11% |
| 4 | 20.191 | 0.57% |
| 5 | 23.040 | 1.76% |
| 6 | 25.448 | 1.92% |
| 7 | 26.581 | 1.18% |
| 8 | 27.637 | 2.04% |
| 9 | 29.541 | 1.50% |

## Analysis of Uncertainty in Each Test

Statistical uncertainty bounds on the measured frequency response function magnitude and phase were computed from the measured coherence functions, assuming that the errors were distributed in a Gaussian manner, according to the following formulas from Bendat and Piersol [20]:

$$\sigma(|H(\omega)|) = \frac{\sqrt{1-\gamma^2(\omega)}}{|\gamma(\omega)|\sqrt{2n_d}}|H(\omega)|$$
$$\sigma(\angle H(\omega)) = \frac{\sqrt{1-\gamma^2(\omega)}}{|\gamma(\omega)|\sqrt{2n_d}}\angle H(\omega) \quad (2)$$

where $|H(\omega)|$ and $\angle H(\omega)$ are the magnitude and phase angle of the measured FRF, respectively, $\gamma^2(\omega)$ is the coherence function, $n_d$ is the number

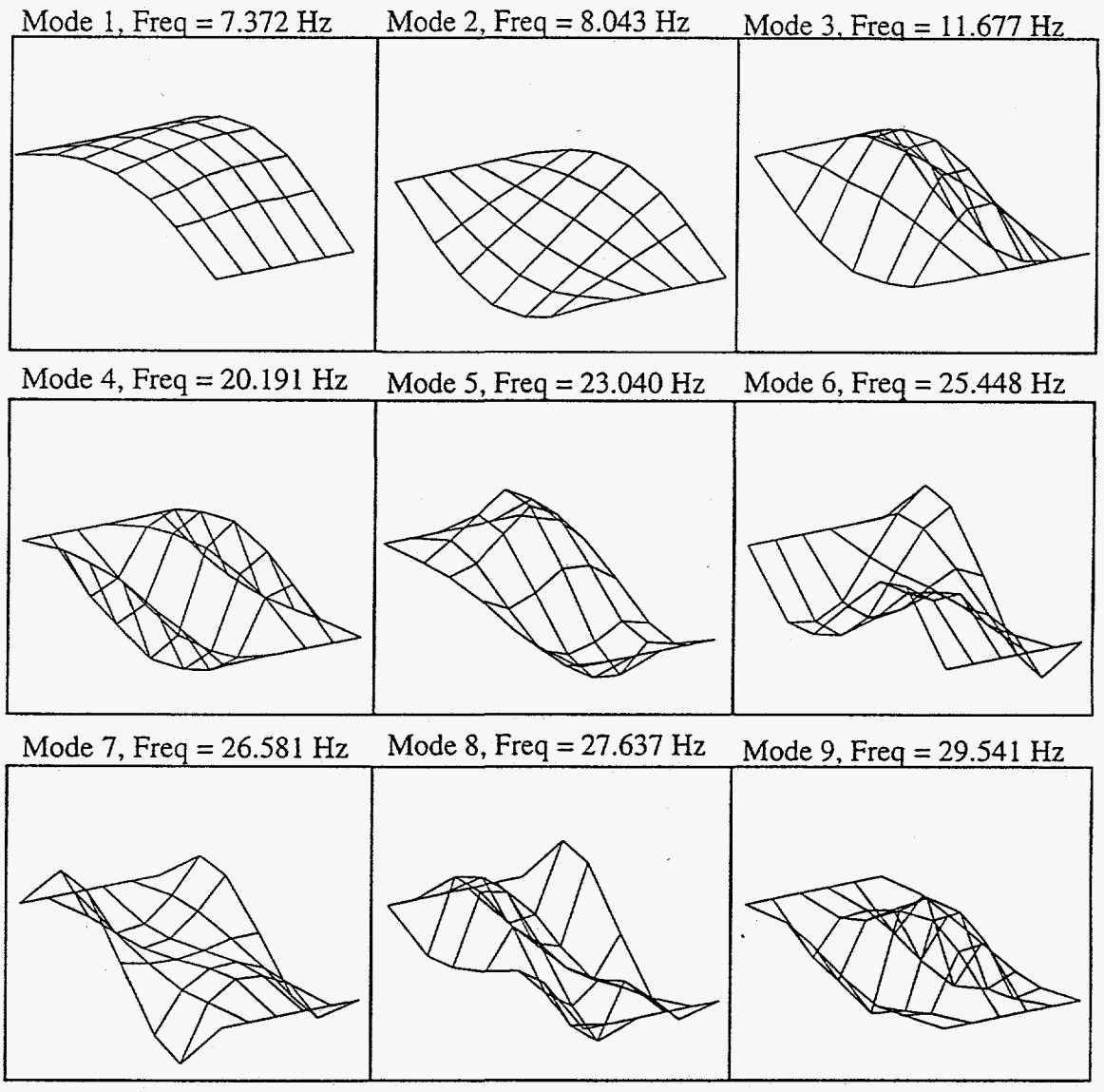


**Figure 10: Identified Mode Shapes for Alamosa Canyon Bridge**

of measurement averages, and $\sigma(\bullet)$ is the value of 1 standard deviation (68% uncertainty bound). These uncertainty bounds represent a statistical distribution of the FRF based on a realistic level of random noise on the measurement. Once the 1 standard deviation (68% uncertainty) bounds were known, 2 standard deviation (95% uncertainty) bounds were computed. Typical 95% uncertainty bounds on the FRF magnitude and phase for this data set are shown in Figure 11.

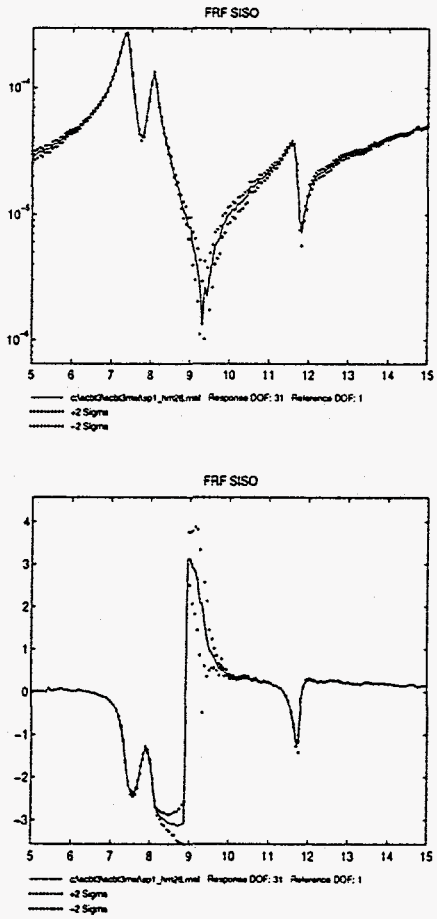


**Figure 11: Typical 95% Confidence Bounds on FRF Magnitude and Phase**

Statistical uncertainty bounds on the identified modal parameters (frequencies, damping ratios, and mode shapes) were estimated using the uncertainty bounds on the FRFs via a Monte Carlo analysis [6]. The basic idea of a Monte Carlo analysis is the repeated simulation of random input data, in this case the FRF with estimated mean and standard deviation values, and compilation of statistics on the output data, in this case the ERA results. For this analysis, the procedure is summarized as:

1. Add Gaussian random noise to the FRFs using the noise standard deviations computed using Eq. (2). This additive noise represents a realistic level of random variations in the measurements.

2. Run the noisy FRF through the ERA identification procedure and apply the modal discrimination using the previously computed parameters.

3. Compute the mean and standard deviation of each modal frequency, damping ratio, and mode shape component over the total number of runs.

4. Repeat steps 1, 2, and 3 until the means and standard deviations calculated in step 3 converge.

For the current study, the convergence took about 100 runs. Tracking the convergence determined the sufficient sample size to provide significant confidence on the statistical estimates. The 95% uncertainty bounds on the modal frequencies, mode shapes, and mode shape curvatures resulting from random disturbances and noise, as computed by the Monte Carlo analysis, are presented in Table 2. These three sets of parameters (frequencies, mode shapes, and mode shape curvatures) were analyzed because they are the parameters most commonly used in damage identification and model refinement analyses. It is observed from these results that the uncertainty bounds on the modal frequencies are much smaller than on the mode shapes, with the mode shape curvatures having the largest uncertainties. (The definition of the "average" errors for mode shape and mode shape curvature are presented in the comparison section of the paper.)

**Table 2. Uncertainty Bounds on Measured Parameters from Random Disturbances**

| Mode # | Error on Modal Freq | Avg. Error on Mode Shape | Avg. Error on Mode Shape Curvature |
|---|---|---|---|
| 1 | 0.06% | 1.68% | 555.49% |
| 2 | 0.73% | 45.42% | 5118.41% |
| 3 | 0.06% | 1.74% | 6.85% |
| 4 | 0.24% | 23.77% | 12.98% |
| 5 | 0.50% | 157.83% | 637.66% |
| 6 | 0.06% | 5.58% | 36.97% |
| 7 | 0.09% | 3.63% | 33.61% |
| 8 | 0.11% | 5.50% | 9.54% |
| 9 | 0.19% | 156.16% | 36.57% |

Analysis of Uncertainty from Environmental Variations

Figure 9 shows the first mode frequencies along with their 95% confi-

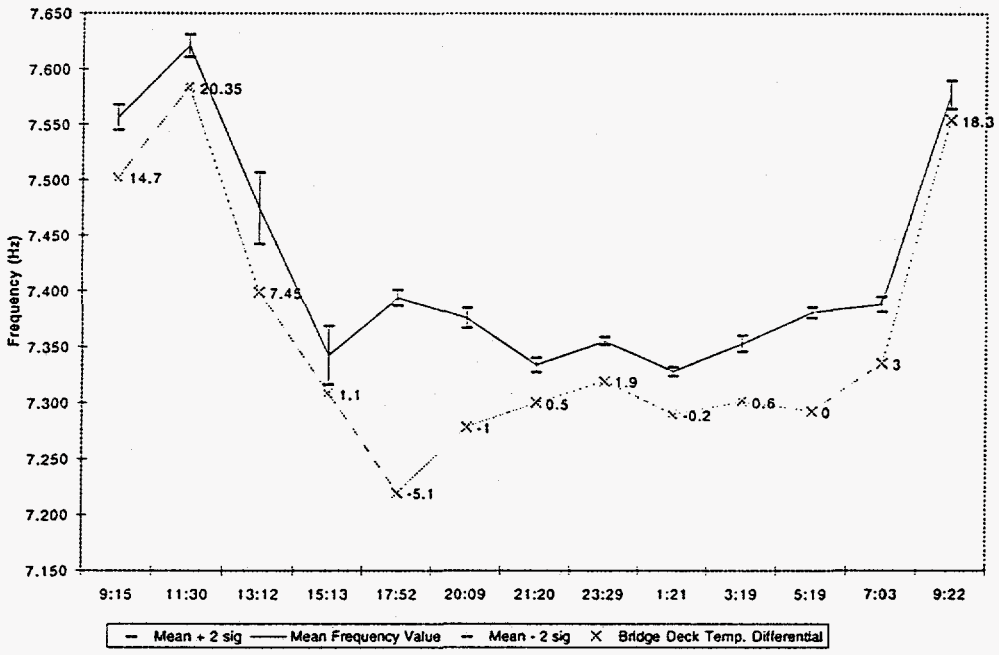


**Figure 12: Changes in First Modal Frequency over a 24 hour Period**

dence limits plotted as a function of the measurement completion time. Also plotted on Fig. 9 is the change in temperature between the two thermometer readings made on the concrete deck (east - west). This figure clearly shows that the change in modal frequencies are related to the temperature differentials across the deck. The first mode frequency varies approximately 5% during this 24 hour time period. Similar variations and correlation with deck temperature differentials were observed for the other modes of the structure.

Effects of Uncertainties on Damage Identification

The changes in the bridge as a result of damage were predicted using the finite element model. The damage case modeled was the 100% failure of a connection between a cross-member and an interior girder. A comparison

of the estimated 95% confidence bounds and the predicted changes as a result of damage for the modal frequencies are shown in Figure 13.The modal

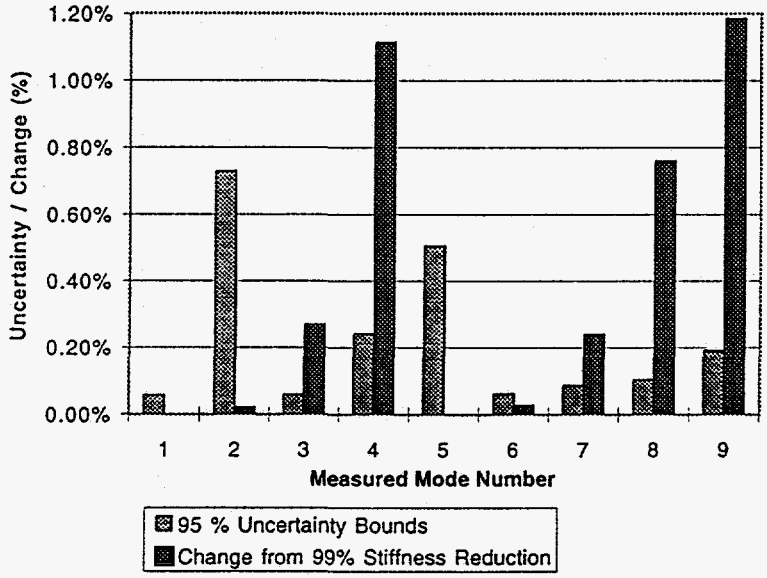


**Figure 13: Comparison of Modal Frequency 95% Confidence Bounds to Changes Predicted as a Result of Damage**

frequencies of modes 3, 4, 7, 8, and 9 undergo a change that is significantly larger than the corresponding 95% confidence bounds. The relative magnitudes of the changes indicate that the frequency changes of these modes could be used with confidence in a damage identification analysis. It should be noted from the y-axis scale of Figure 13 that the overall changes in frequency as a result of damage are quite small (< 1.2%), but as a consequence of the extremely low uncertainty bounds on the modal frequencies (many less than 0.2%), these small changes can be considered to be statistically significant.

The relative statistical significance of the changes in the various modes is one of the primary motivating factors for the selective flexibility approach. Using the selective flexibility, those modes where the frequency changes are statistically insignificant would be considered to be unchanged, while those modes with significant frequency change would be used in the flexibility analysis.

One method for comparison of the confidence bounds on the mode

shape components to the predicted change as a result of damage is a direct, component-by-component comparison. Such a comparison for modes 3 and 7 is shown in Figure 14. These plots show the mean values of the undam-

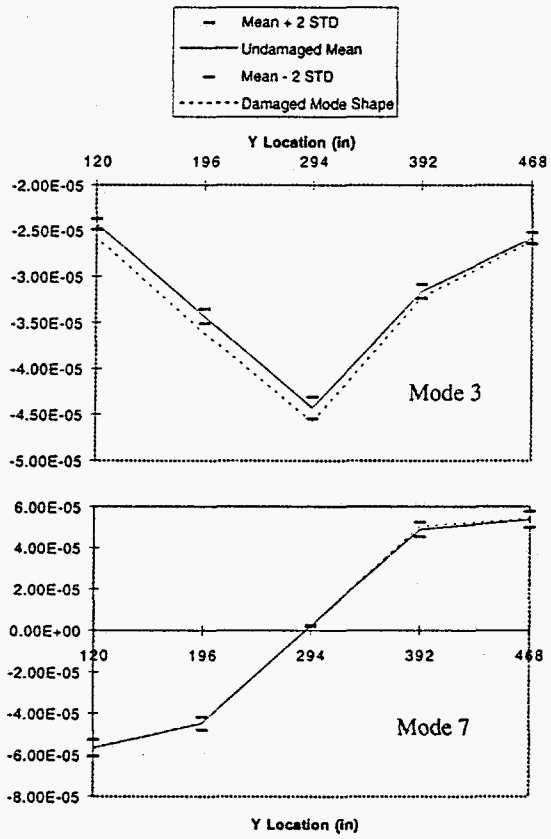


**Figure 14: Comparison of Modes 3 and 7 Confidence Bounds and Predicted Change After Damage**

aged mode shape components in a solid line (with 95% confidence bounds at the measurement locations), with the predicted mode shape after damage represented by a dashed line. These mode shape components represent a "slice" of each of these mode shapes taken along one girder of the bridge. This slice of mode shape 3 contains 3 components that have a predicted change from damage that is greater than the 95% confidence bounds. Thus, the change in these 3 components can be used with confidence in a damage identification algorithm. However, none of the components of this slice of mode shape 7 have a change that is greater than the 95% bound, so these components of this mode shape have an insignificant change as a result of damage, and should not be used in a damage identification analysis

## CONCLUSION

A new toolbox of graphical-interface software algorithms, known as DIAMOND, has been introduced and demonstrated. The toolbox provides the capability to simulate vibration tests, perform experimental modal analysis including statistical bounds, apply various damage identification techniques, and implement finite element refinement algorithms. The structure of the toolbox menus was described in detail in this paper, and a sample application to measured data from a highway bridge was presented.

## ACKNOWLEDGMENTS

This work was supported by Los Alamos National Laboratory Directed Research and Development Project #95002, under the auspices of the United States Department of Energy. The authors wish to recognize the contributions of Mr. Erik G. Straser and Mr. A. Alex Barron of Stanford University.

## REFERENCES

1. MATLAB, *Users Manual*, The Mathworks, Inc., 1994.

2. Juang, J.N. and Pappa, R.S., "An Eigensystem Realization Algorithm for Modal Parameter Identification and Model Reduction," *Journal of Guidance, Control and Dynamics*, Vol. 8, No. 5, pp. 620-627, 1985.

3. Vold, H., Kundrat, J., Rocklin, T., and Russell, R., "A Multi-Input Modal Estimation Algorithm for Mini-Computers," SAE Transactions, Vol. 91, No. 1, January 1982, pp. 815-821.

4. Richardson, M.H. and Formenti, D.L., "Parameter Estimation from Frequency Response Measurements using Rational Fraction Polynomials," *Structural Measurement Systems Technical Note 85-3*, 1985.

5. McVerry, G.H., "Structural Identification in the Frequency Domain from Earthquake Records," Earthquake Engineering and Structural Dynamics, Vol. 8, 1980, pp.161-180.

6. Press, W.H., Teukolsky, S.A., Vetterling, W.T., and Flannery, B.P., *Numerical Recipes in FORTRAN: The Art of Scientific Computing*, Sec-

ond Edition, Cambridge Univ. Press, 1992, pp. 684-686.

7. Stubbs, N., J.-T. Kim, and C.R. Farrar, 1995, "Field Verification of a Nondestructive Damage Localization and Severity Estimation Algorithm," in *Proc. 13th International Modal Analysis Conference*, 210–218.

8. Cornwell, P., Doebling, S.W., and Farrar, C.R., "Application of the Strain Energy Damage Detection Method to Plate-Like Structures," to appear in *Proc. of the 15th International Modal Analysis Conference*, Orlando, FL, February, 1997.

9. Catbas, F.N., Lenett, M., Brown, D.L., Doebling, S.W., Farrar, C.R., and Turer, A., "Modal Analysis of Multi-Reference Impact Test Data for Steel Stringer Bridges," to appear in *Proc. of the 15th International Modal Analysis Conference*, Orlando, FL, February, 1997.

10. Robinson, N.A., L.D. Peterson, G.H. James, and S.W. Doebling, 1996, "Damage Detection in Aircraft Structures Using Dynamically Measured Static Flexibility Matrices," in *Proc. of the 14th International Modal Analysis Conference*, 857–865.

11. Doebling, S.W., Peterson, L.D., and Alvin, K.F., "Estimation of Reciprocal Residual Flexibility from Experimental Modal Data," AIAA Journal, Vol. 34, No. 8, pp. 1678–1685, August 1996.

12. Doebling, S.W., Farrar, C.R., Prime, M.B., and Shevitz, D.W., "Damage Identification and Health Monitoring of Structural and Mechanical Systems From Changes in Their Vibration Characteristics: A Literature Review," Los Alamos National Laboratory report LA-13070-MS.

13. Zimmerman, D.C. and M. Kaouk, 1994, "Structural Damage Detection Using a Minimum Rank Update Theory," *Journal of Vibration and Acoustics*, **116**, 222–230.

14. Doebling, S.W., "Damage Detection and Model Refinement Using Elemental Stiffness Perturbations with Constrained Connectivity," in *Proc. of the AIAA/ASME/AHS Adaptive Structures Forum*, pp. 360–370, AIAA-96-1307, 1996. Accepted and to appear in *AIAA Journal*.

15. Baruch, M., 1982, "Optimal Correction of Mass and Stiffness Matrices Using Measured Modes," *AIAA Journal*, 20(11), 1623–1626.

16. Hemez, F.M. and C. Farhat, 1995, "Structural Damage Detection via a Finite Element Model Updating Methodology," *Modal Analysis: The International Journal of Analytical and Experimental Modal Analysis*, **10** (3), 152–166.

17. Alvin, K.F., 1996, "Finite Element Model Update via Bayesian Estimation and Minimization of Dynamic Residuals," in *Proc. of the 14th International Modal Analysis Conference*, 561–567.

18. Ricles, J.M. and J.B. Kosmatka, 1992, "Damage Detection in Elastic Structures Using Vibratory Residual Forces and Weighted Sensitivity," *AIAA Journal*, **30**, 2310–2316.

19. Farrar, C.R., Doebling, S.W., Cornwell, P.J., and Straser, E.G., "Variability Of Modal Parameters Measured On The Alamosa Canyon Bridge," to appear in *Proc. of the 15th International Modal Analysis Conference*, Orlando, FL, February, 1997.

20. Bendat, J.S. and Piersol, A.G., *Engineering Applications of Correlation and Spectral Analysis*, John Wiley and Sons, New York, 1980, p. 274.

21. Farhat, C. and Hemez, F. M., "Updating Finite Element Dynamic Models Using an Element-By-Element Sensitivity Methodology," *AIAA Journal*, Vol. 31, No. 9, September 1993, pp. 1702-1711.

22. Alvin, K.F., 1996, "Finite Element Model Update via Bayesian Estimation and Minimization of Dynamic Residuals," in *Proc. of the 14th International Modal Analysis Conference*, 561–567.

23. Ricles, J.M. and J.B. Kosmatka, 1992, "Damage Detection in Elastic Structures Using Vibratory Residual Forces and Weighted Sensitivity," *AIAA Journal*, **30**, 2310–2316.